Journal of Magnetic Resonance 192 (2008) 323–328

Contents lists available at ScienceDirect

Journal of Magnetic Resonance

journal homepage: www.elsevier.com/locate/jmr

# Capillary scale NMR flow mapping

Walter Massefski

*Department of Chemical Technologies, Chemical and Screening Sciences, Wyeth Research, 200 CambridgePark Drive, Cambridge, MA 02140, USA*

ARTICLE INFO

*Article history:*
Received 6 August 2007
Revised 14 March 2008
Available online 21 March 2008

*Keywords:*
Microsample NMR
Flow NMR
Capillary NMR

ABSTRACT

Stopped-flow NMR at capillary scale has many advantages over traditional methods of introducing the sample into the probe, particularly when large numbers of samples must be examined. This work describes application of a simple method for direct visualization of a sample inside the flow cell of flow NMR systems to capillary scale analysis. We describe the details of the method and show how it can be used to measure the optimum flow rate for a capillary NMR system and how to determine the optimum sampling efficiency for small samples.



## 1. Introduction

Flow NMR systems are generally used in stopped-flow mode, in which the sample is moved by pumped carrier solvent to the NMR probe and stops for analysis. This approach depends critically on correct placement of the sample of interest in the center of the NMR coil/NMR flow cell. This is particularly important at the very small volumes of capillary NMR [1,2], since an error of a few microliters can lead to a significant decrease in the observed NMR signal. In capillary NMR systems, one approach is to carefully calibrate the system with a series of experiments that gradually increment the flow length and plot this length versus signal (or S/N) to determine the optimum parameters for the system. This approach allows for an accurate determination of the sample parking volume, but it is somewhat slow, being limited by the time required for a complete transit through the flow system.

This process is reasonably straightforward when the system is to be used with a single solvent, a single flow path, a single pump, etc., but it tends to provide a barrier to flexible use of the flow system because the time required for calibration may be a significant fraction of the run time for each state of the system. We were interested in developing a simple method that could be used to reliably determine both the push volume and the wash volume of a capillary NMR system under a variety of solvent and flow conditions.

One of the goals of this paper is to make capillary scale flow NMR as accessible as conventional flow NMR. Since the instrumentation has been available to the NMR community for a relatively short period of time, many of the principles for routine use of these systems have not been fully established. In particular, discussions with colleagues about capillary flow suggests that only a small fraction of those who have purchased systems have been successful in their implementation, and we hoped to elucidate a practical strategy which allow scientists to fully utilize these methods. Although it is true that flow is flow, the difference in flow rates and volumes, tubing diameters, and sample sizes results in a much more plug-like flow behavior of capillary systems relative to the mixing-type behavior of standard flow systems. Therefore, we have attempted to describe the characteristics of capillary flow systems in some detail.

Flow mapping with NMR detection has been employed for a variety of applications, most notably in MRI angiography, NMR microscopy, and NMR rheography [3–5]. These methods focus on the properties of the flowing stream and typically employ spatial localization techniques. Our need is for a much simpler tool to examine the average behavior of the flow system, rather than the details of that system. In addition, we are interested in optimum handling of material-limited samples, where a fixed and small amount of sample is available for study [6,7]. This is often the case for natural product or other biological materials and for combinatorial chemistry samples that are synthesized at the sub-milligram level [8,9]. We present here a flow mapping method that allows for easy optimization of capillary flow NMR systems at the sub-milligram sample level. Examples of on-flow monitoring have been applied to analytical scale flow NMR and methodology can be found in instrument vendor manuals; here we have extended this approach to capillary scale.

## 2. Experimental

All experiments were performed on a Bruker AV400 NMR system (Bruker BioSpin Inc.) equipped with a capNMR flow probe

*E-mail address:* wmassefski@wyeth.com

1090-7807/$ - see front matter © 2008 Elsevier Inc. All rights reserved.
doi:10.1016/j.jmr.2008.03.008

(Protasis Corp.). The flow probe in our system has a 5 μl flow cell (the active NMR volume of the system is 2.5 μl). The system is driven with a LEAP autosampler and a single Protasis HTSL pump in single solvent mode. We observe back pressures in the range of 1000 psi at 40 μl/min operating flow rates. All solvents are filtered in-line. Deuterated solvents for push and NMR acquisition are standard bottle grade (>99.5% *D*) from Cambridge Isotope Laboratories.

The simplest system for introducing a sample into a capillary flow probe is to use a microliter syringe to push sample into the probe inlet, but this is not the most convenient, reliable, or sample conservative approach. Our system is equipped with a LEAP autosampler for full-automation use, and we have found that the most convenient method for introducing samples into the probe in low-throughput mode involves direct injection of the sample from a manual microliter syringe into the LEAP sample loop, followed by a push from the HTSL pump to get the sample to the probe. This approach allows for easy calibration of push volume at a variety of flow rates and injection loop sizes. The manual injection volume can be nearly the same as the volume of the injection loop, minimizing loss of sample at the injection stage. The push volume is empirically measured by the approach outlined in this work, but it is largely determined by the volume of tubing between the injection valve and the probe and the size of the injection loop. We have used 0.004″ ID FEP tubing (Upchurch Scientific) throughout in this work, but other sizes (as well as PEEK tubings) are possible as well, and several have been evaluated in the course of this work.

NMR experiments for fast flow acquisition were performed in 2Dser mode (consecutive 1 D NMR traces are stored in a 2D file, processed in one dimension, and displayed 2D). This method has been employed for non-capillary flow NMR systems, and detailed methods can be found in vendor LC-NMR manuals. Capillary flow rates of up to 60 μl/min (1 μl/s) can be accommodated with one scan per increment times 1024 increments, short acquisition times (0.285 s) and short relaxation delays (40 ms) with small flip angle pulses (about 5 degrees). Under these conditions our time resolution is 3 increments/s, which allows for the resolution shown in Table 1.

Even at the fastest flow rate, this resolution is sufficient for accurate measurement of the flow characteristics of the system. The combination of one scan per increment and small flip angles requires a highly concentrated sample, yet it is important for the test conditions to accurately reflect operating conditions for real samples; in particular we need our calibration method to have the same solvent flow characteristics as those of a real sample. We found the best compromise is a moderate concentration of protonated solvent mixed in the deuterated lock solvent of choice. This obviates the need for sample specific setup, such as presaturation of solvent resonances, while maintaining the necessary solvent flow characteristics.

These strong samples have the added bonus that it is quite easy to see what the necessary wash out volume must be, and relaxation from radiation damping helps with our short relaxation delays [10]. Samples are injected into a fixed volume sample loop, then pushed into the probe with the HTSL pump. The sample loop size would typically be somewhat greater than the flow cell size (approximately 8 μl for a 5 μl flow cell), although this can be reduced to achieve greater sampling efficiency. The sample loop size in indicated with the experiments below. Data can be visualized either directly by 2D plot (see Fig. 1 as an example) or as the projection of the 2D data along the time axis, as shown in Fig. 6.

**Table 1**
Effect of flow resolution on-flow rate

| Flow rate (μl/min) | Resolution (μl/increment) |
|---|---|
| 60 | 0.333 |
| 40 | 0.222 |
| 20 | 0.111 |
| 10 | 0.056 |
| 5 | 0.028 |

## 3. Results and discussion

We show an example of a flow experiment in Fig. 1. In this experiment, a 5 μl sample loop is filled with sample, and the sample is pushed through the flow cell. We can see the sample enter the flow cell after a time that is related to the flow path length leading up to the flow cell, in this case approximately 30 μl. Once the sample begins to enter the flow cell it mixes with solvent in the flow cell until it reaches a maximum NMR signal 7.5 μl after the sample first enters the flow cell. After this time the sample begins to sweep through the flow cell and out of the probe. At approximately 20 μl after the sample first enters the flow cell, the sample has completely left it, suggesting that four cell volumes are sufficient under these flow conditions to remove the sample from the flow cell. If the NMR experiment is synchronized with the start of the delivery pump it is possible to determine the ideal delivery volume in a single 5-min experiment; the ideal delivery volume is calculated from the row number and the volume resolution given in Section 2, and has shown to be reproducible to within one- or two-tenths of 1 μl at the lower flow rates. This delivery volume can be used directly to deliver a mass-limited sample to the flow cell to achieve the greatest NMR sensitivity.

The 2D plot makes it particularly easy to visualize what is happening to the sample as it flows through the cell. In a typical experiment we would expect to load the sample loop, deliver the sample in the loop to the probe with a fixed volume of push solvent, acquire NMR data on the sample, and finally push the sample out of the probe to make it ready for the next sample. In Fig. 2, we have delivered the sample with a push volume that is (a) too large, (b) too small, or (c) just right. In Fig. 2a, the ideal delivery volume is less than the actual delivery volume used; therefore the maximum observed signal decreases to a steady-state when the sample is parked. In Fig. 2b, the maximum possible signal (maximum possi-

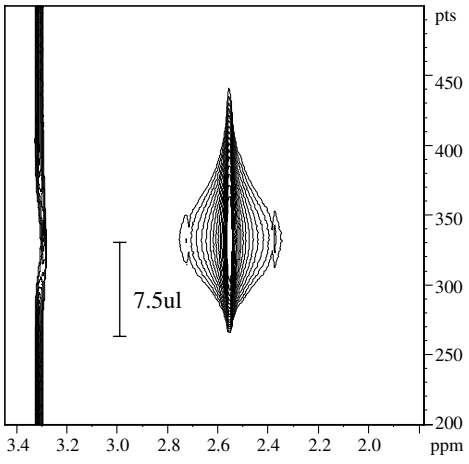


**Fig. 1.** A sample of 25% DMSO in $d_6$-DMSO was placed in a 5 μl injection loop (the loop was overfilled to insure complete sample introduction) and pushed through the capNMR flow probe with 100 μl $d_6$-DMSO push solvent at 20 μl/min. The signal maximum occurred at approximately scan 325 (out of 1024), or 23 μl from the sample loop.

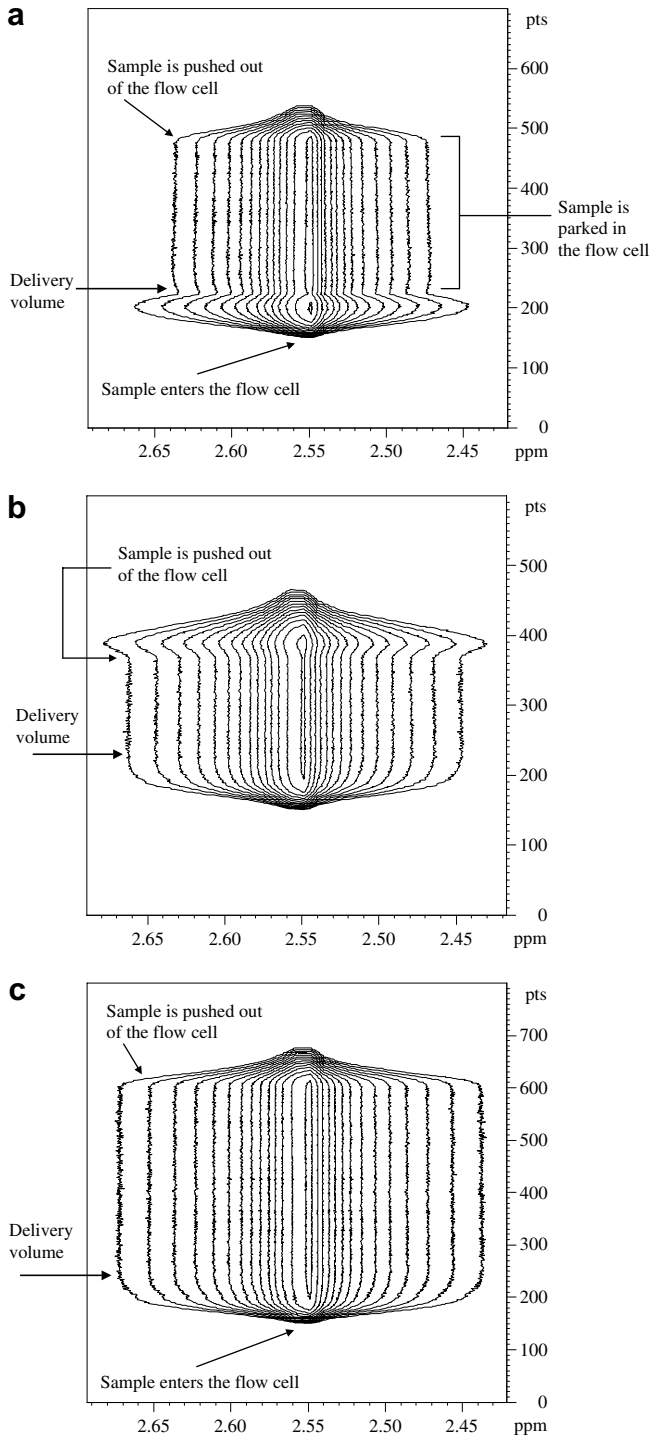


**Fig. 2.** Each experiment was run under the same conditions as in Fig. 1, except that the sample was parked at (a) 25 μl, (b) 21 μl, and (c) 23 μl from the sample injection loop. All display conditions are identical.

ble filling of the flow cell with the sample) occurs as the sample is pushed out of the flow cell. Only in Fig. 2c, when the appropriate delivery volume is used, is the maximum signal intensity achieved when the sample is parked.

Many applications of this approach can be imagined, from optimizing the system for different solvents to changing operating conditions, tubing, flow cells, etc. We wished to ask a particularly practical question: what is the optimum flow rate for the system? If the sensitivity is the same at all flow rates then faster is better, because it leaves more time for NMR data acquisition, but as we see in Fig. 3, the maximum sensitivity is a strong function of the delivery flow rate in the range 5–60 μl/min. Most of this difference in sensitivity is due to the mixing that occurs between the sample and the solvent just ahead of it in the flow cell, which is much greater at higher flow rates. The difference in intensity between the slowest and fastest rate is threefold and essentially monotonic up to 40 μl/min (see Fig. 4), which means that the optimum experimental conditions will be a balance between slow delivery rates (to increase total signal strength) and fast delivery rates (to give the sample more time in the probe). Since the sensitivity term is expected to follow a square root law we expect that it will dominate, particularly for weaker samples. As we see in Fig. 5, this is the case: the optimum delivery rate decreases from 30 μl/min for strong samples (samples where we expect to get good S/N in 1 min) down to 10 μl/min for weak samples. The range of sample delivery times for a typically configured capillary system will be between 0.5 and 5 min between the fastest and slowest flow rates,

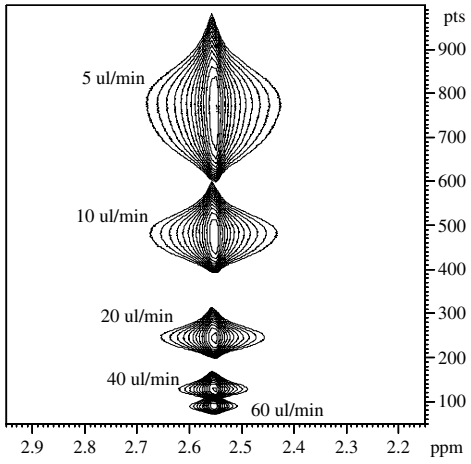


**Fig. 3.** This plot shows a superposition of five separate experiments of the type described in Fig. 1 at five different flow rates. The 60, 40, 20, and 10 μl/min acquisitions were synchronized with the delivery pump; the 5 μl/min acquisition started 1 min after the pump was turned on.

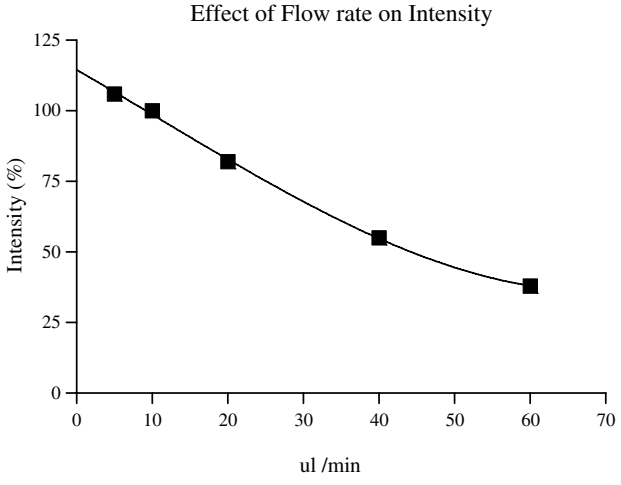


**Fig. 4.** The maximum intensity trace from each experiment in Fig. 3 was extracted and integrated to produce this figure. The 10 μl/min point was set arbitrarily to 100%.

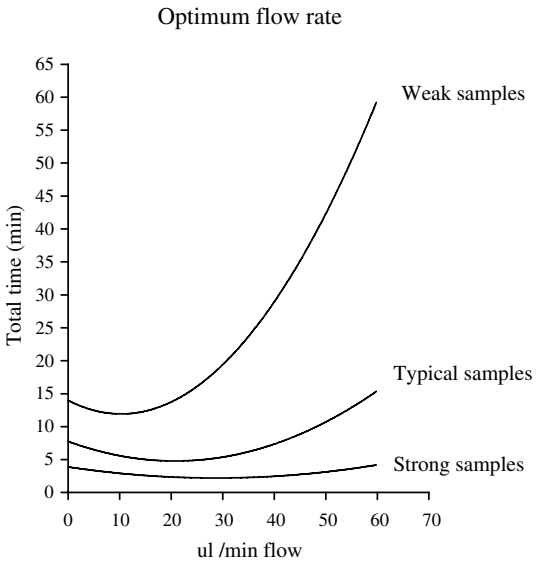


**Fig. 5.** Timings were calculated by assuming typical small molecule 1D proton NMR conditions, total scan time of 4 s. The strong sample was assumed to give a good spectrum in 8 scans at 10 μl/min flow delivery; for typical and weak samples these were 32 scans and 128 scans, respectively. Inject times were calculated from the signal maximum observed in Fig. 3, which varied between 26 and 30 μl, and acquisition times were calculated based on the relative maximum signal intensities observed in the same experiments. We assumed the sample eject rate would be the same for all experiments and would be independent of the sample delivery rate.

respectively. The acquisition times to achieve equivalent sensitivity at optimal versus sub-optimal flow rates can be nearly an hour for weaker samples.

This flow mapping method also allows us to explore the optimum injection size for mass-limited samples. When a fixed quantity of sample is available for study, it is critical that we waste as little as possible getting the sample to the probe, so that we have as much as possible left for NMR analysis. It is also quite important that we introduce the sample into the probe in a reliable way; there is nothing worse than losing an entire small sample before having a chance to study it.

Fig. 6 shows the effect of injection size on the observed NMR signal intensity. The experiment in Fig. 6 shows that at constant sample concentration, both the height and the width of the maximum are affected by the sample size (the volume of the sample injection loop). At injection volumes that are less than the flow cell size, the peak is relatively narrow, and the total signal is a strong function of the injection volume (see Fig. 7). At injection volumes that are greater than the flow cell size, the maximum signal reaches a plateau that is only slightly greater than that observed for a 5 μl loop size (the flow cell is also 5 μl). Fig. 8a shows how this translates to the efficiency of sampling a fixed amount, rather than a fixed concentration of sample. In this experiment approximately 40 micrograms of adenosine is dissolved in varying amounts of solvent, then injected into an equivalently sized sample injection loop. The optimum sampling efficiency is achieved when the sample volume is equal to the flow cell size. Samples that are larger than this dilute the sample, and therefore show lower signal to noise (see Fig. 8b). Samples that are smaller should, in principle, exhibit the same efficiency as samples that are equal in size to the flow cell, but they tend to suffer from the practical problems associated with introducing very small samples into the probe, such as dilution of the sample in the syringe.

The reliability of the injection technique is implied by the width of the peak in Fig. 6. At smaller injection volumes the push volume must be defined fairly precisely, whereas larger samples are more easily delivered to the probe flow cell. If we define the 'misset tolerance' of the system by the range of volumes that give signal within 10% of the maximum, then we can depict this as shown in Fig. 9. The misset tolerance for a 5 μl sample in this system is ±2 μl, a fairly wide range of push volumes. We believe this misset tolerance is generous enough to easily adapt this method to automation.

Finally, we can show the sampling efficiency of the system in Fig. 10. The sampling efficiency can be no more than 0.5, since the RF coil only detects half of the flow cell, but this efficiency is decreased for small samples because of the sample preparation issues discussed above. The sampling efficiency decreases for larger samples because some of the sample is outside the flow cell.

## 4. Conclusions

We have developed a capillary NMR flow mapping approach which allows us to easily compare different operating conditions and gives a simple measure to optimize the sensitivity of such a system. Since system optimization is typically a slow process,

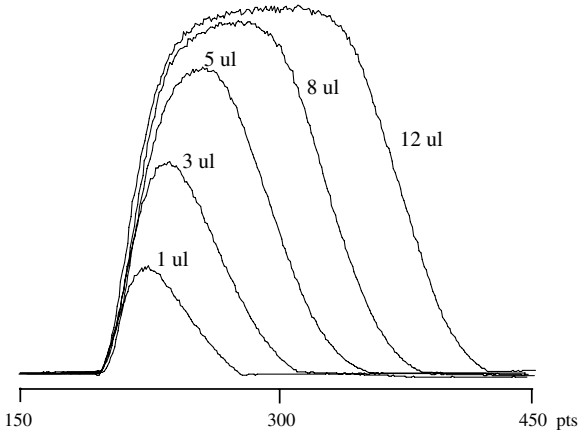


**Fig. 6.** These traces are the projection of the total sample intensity along the time axis for the type of experiment shown in Fig. 1. Results for injection loops of 1 μl, 3 μl, 5 μl, 8 μl, and 12 μl are shown, all at 20 μl/min flow rate. The sample was 25% DMSO in $d_6$-DMSO. Since the majority of the signal in the sample is from the protonated DMSO and the background signals are constant over all the experiments, it is possible to compare the absolute intensities of the projections to each other.

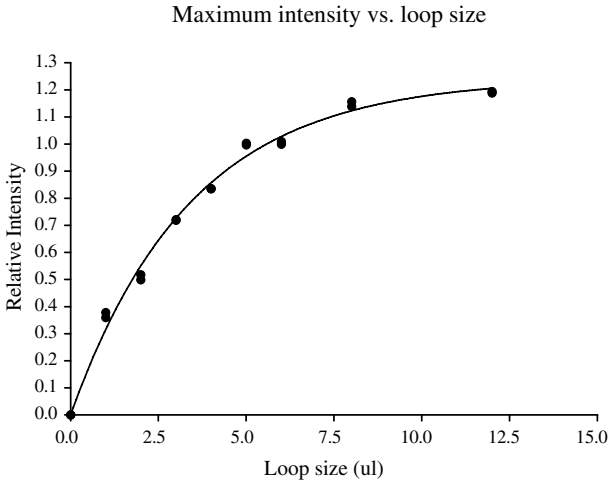


**Fig. 7.** This figure shows the maximum intensity observed for a 25% DMSO in $d_6$-DMSO sample as a function of injection loops size in the range 1–12 μl. The average intensity of the 5 μl samples was arbitrarily set to 1.0.

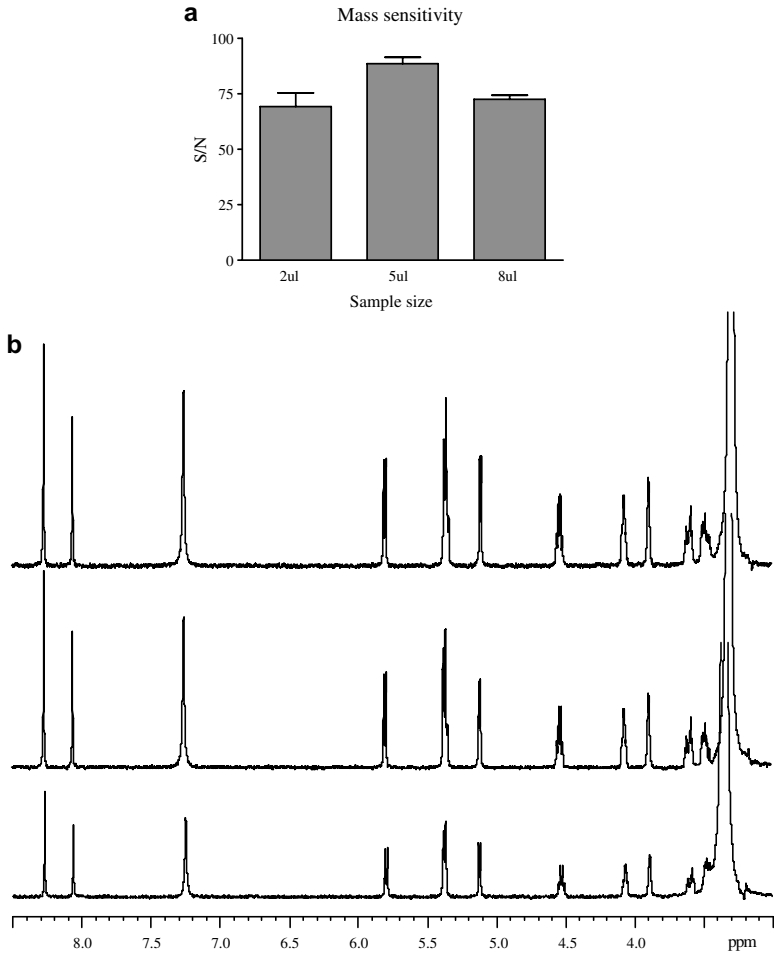


**Fig. 8.** (a) This graph shows the mass sensitivity of the system at 20 μl/min flow rate as a function of sample size. 1 μl of 145 mM adenosine in $d_6$-DMSO (38.75 μg adenosine) was diluted with the appropriate amount of $d_6$-DMSO to achieve the final sample size, which was then loaded into the injection loop manually with a 25 μl Hamilton syringe. The syringe and sample loop were washed between experiments. The push volume was determined for each sample loop with a single experiment of the type shown in Fig. 1, followed by either 3 (for the 2 μl and 8 μl experiments) or 5 (for the 5 μl experiment) replicates of a typical 8 scan proton 1D observe. The bar graph shows the mean and standard error of the measurement. (b) This is NMR data for the points shown in Figure 8a. Each trace is for a single sample using a 2 μl (bottom), 5 μl (middle), or 8 μl (top) injection of 38.75 μg adenosine in $d_6$-DMSO.

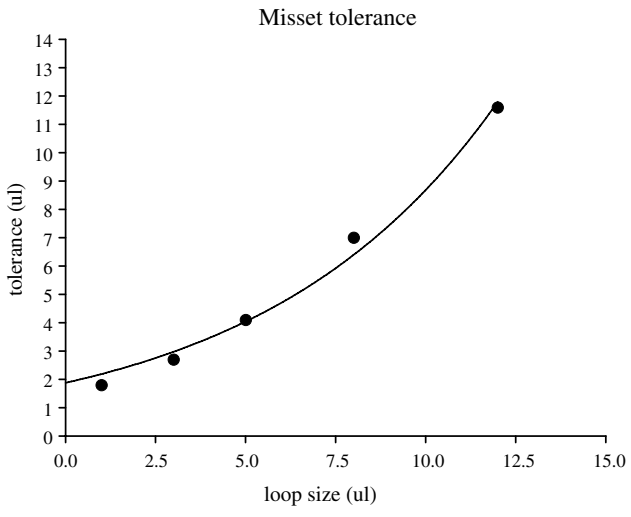


**Fig. 9.** This graph shows the effect of the injection loop size on the misset tolerance. The misset tolerance is defined as the range of volumes that give signal within 10% of the maximum, and is defined in microliters. For example, the observed misset tolerance at 5 μl injection volume is 4.1 μl, which means that if we are within ±2 μl of the correct push volume we will stay within 90% of the maximum NMR signal intensity.

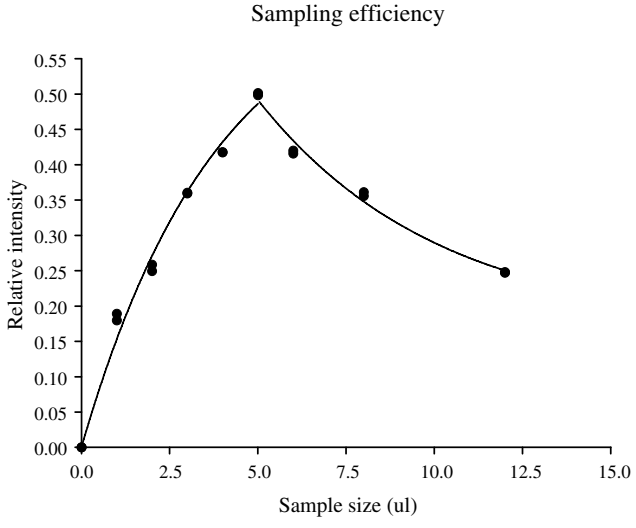


**Fig. 10.** This is a graph of the sampling efficiency for the system using a constant concentration sample. The initial part of the graph is determined by the maximum sensitivity for each loop size as shown in Fig. 7, scaled by 50%. Points for samples >5 μl are multiplied by the fraction of the injected sample that actually resides in the flow cell. In the limit of perfect sample handling of fixed-mass samples, the sampling efficiency for samples less than or equal to 5 μl would all be the same.

capillary flow systems are rarely used to their full potential. This method overcomes that barrier.

## Acknowledgments

We thank Aaron Wilson and Dean Olson of Protasis/MRM for many useful and important discussions about capillary NMR flow behavior which helped to guide the development of this method. We also acknowledge Oliver McConnell for his support of this research.

## References

[1] D.L. Olson, J.A. Norcross, M. O'Neil-Johnson, P.F. Molitor, D.J. Detlefsen, A.G. Wilson, T.L. Peck, Microflow NMR: concepts and capabilities, Anal. Chem. 76 (2004) 2966–2974.
[2] F.C. Schroeder, M. Gronquist, Extending the scope of NMR spectroscopy with microcoil probes, Angew. Chem., Int. Ed. 45 (2006) 7122–7131.
[3] J. Zuo, M. Bolding, D.B. Twieg, Validation of V-SS-PARSE for single shot flow measurement, Magn. Reson. Imaging 25 (2007) 335–340.
[4] E. Kossel, R. Kimmich, Flow measurements below 50 μm: NMR microscopy experiments in lithographic model pore spaces, Magn. Reson. Imaging 23 (2005) 397–400.
[5] T. Baumann, R. Petsch, R. Niessner, Direct 3-D measurement of the flow velocity in porous media using magnetic resonance tomography, Environ. Sci. Technol. 34 (2000) 4242–4248.
[6] R.A. Kautz, W.K. Goetzinger, B.L. Karger, High-throughput microcoil NMR of compound libraries using zero-dispersion segmented flow analysis, J. Comb. Chem. 7 (2005) 14–20.
[7] R.A. Kautz, M.E. Lacey, A.M. Wolters, F. Foret, A.G. Webb, B.L. Karger, J.V. Sweedler, Sample concentration and separation for nanoliter-volume NMR spectroscopy using capillary isotachophoresis, J. Am. Chem. Soc. 123 (2001) 3159–3160.
[8] A. Jansma, T. Chuan, R.W. Albrecht, D.L. Olson, T.L. Peck, B.H. Geierstanger, Automated microflow NMR: routine analysis of five-microliter samples, Anal. Chem. 77 (2005) 6509–6515.
[9] N.J.C. Bailey, I.R. Marshall, Development of ultrahigh-throughput NMR spectroscopic analysis utilizing capillary flow NMR technology, Anal. Chem. 77 (2005) 3947–3953.
[10] V.V. Krishnan, Radiation damping in microcoil NMR probes, J. Magn. Reson. 179 (2006) 294–298.